

## CHAPITRE 3

### TESTING OF SUPERELASTIC RECENTERING PRE-STRAINED BRACES FOR SEISMIC RESISTANT DESIGN<sup>2</sup>

#### 3.1 Introduction

Traditionally, earthquake damage has been mitigated by designing building structures with the ability to deform in a ductile manner. However, it is often at the cost of large inelastic deformations which can lead to damage. This damage can result in significant permanent deformation and large repair costs. Recent earthquakes including the 1994 Northridge Earthquake in the United States, the 1995 Hyogoken-Nanbu (Kobe) Earthquake in Japan, and the 1999 Kocaeli Earthquake in Turkey have demonstrated some of these deficiencies in building structures and have resulted in significant economic losses. In order to address these problems, the structural engineering community has made considerable efforts to understand the past performance of structures and develop control systems to reduce inelastic deformations in critical structural members. Performance-based design criteria limits inter-story drifts to given seismic design levels. The use of passive and active systems such as base isolators, metallic yield dampers, tuned mass dampers, and friction type dampers are some examples of current practices to control the response of structures and reduce permanent deformations [78]. However, there exists an ever increasing need to develop new systems which can improve the performance of building structures during an earthquake.

SMA's are a class of material that possess the unique ability to return to their original shape even after reaching strain levels of up to 8%. This shape recovery can occur through either the shape memory effect, which requires the application of heat, or

---

<sup>2</sup> Cet article a été accepté pour publication dans le « Journal of Earthquake Engineering » [5]. Les auteurs sont Pierre Lafortune (ÉTS), Jason McCormick (Georgia Tech), Reginald DesRoches (Georgia Tech) et Patrick Terriault (ÉTS).

through the superelastic effect, which only requires the removal of the load. During deformation, SMAs undergo a solid-to-solid diffusionless phase transformation which is completely reversible allowing for the shape to be recovered. In addition to this recentering capability associated with the shape recovery, SMAs have been shown to have stable hysteretic behavior when mechanically trained, provide supplemental energy dissipation, have excellent corrosion resistance, and good fatigue properties which make them strong candidates for seismic applications in the design and retrofit of building structures.

The ability of SMAs to control vibrations has been extensively studied leading to many innovative applications [19;21;58;63]. SMA devices have been installed in the 'San Francesco Basilica Superior' in Italy [67] and DesRoches and Delemont [65] have investigated the effectiveness of SMA restrainer bars to reduce the seismic vulnerability of bridges. Despite these studies, some particular aspects regarding the use of SMAs for seismic applications, such as the effect of pre-staining, are still not well understood.

In the present study, the behavior of superelastic SMAs and their applicability to earthquake engineering applications is explored via the use of a small-scale shake table. First, the material behavior of superelastic SMA wire is studied under loading rates and strain levels equivalent to that expected to be undergone by structural members during an earthquake. The effectiveness of SMA braces to reduce the seismic response of a small-scale frame is then studied. A finite element model (FEM) of the structure studied on the small-scale shake table is developed and validated. Finally, the effect of pre-staining the SMA wires is studied experimentally using the small-scale frame and then studied analytically to gain a better understanding of the brace and system behavior.

### 3.2 Mechanical Behavior of the NiTi Wires

In order to implement SMAs into seismic applications, their behavior under a loading typical of a seismic event must first be understood. The superelastic NiTi wires used for these tests have a diameter of 0.254 mm and are the same as those which are used for the subsequent bracing study of the small-scale frame. The specimens are straight annealed and have a black oxide surface. No additional processing is performed prior to testing. Dynamic tests at 0.5 Hz, 1.0 Hz, and 2.0 Hz are carried out on the wires to determine how loading rates and strain levels equivalent to those experienced by structural members during an earthquake affect the mechanical behavior. The tensile loading protocol used simulates a far-field type earthquake. It consists of one cycle to 0.5% strain, cycles of 1.0%-5.0% strain by increments of 1%, six cycles to 6% strain, and four cycles to 7% strain. An electromagnetic table-top testing apparatus is used in displacement control to implement the loading protocol. Strains are calculated by dividing the cross-head displacement by the gage length, approximately 38.1 mm, since the specimen is too small for the available extensometers. Loads are measured with a 48.9 N load cell.

The stress-strain results for the specimens tested at 0.5 Hz and 1.0 Hz are shown in figure 39. For all of the dynamic loading rates, good superelastic behavior is obtained with a clear flag-shape hysteresis and recovery of the initial shape. The loading plateau stress is found to be unaffected by the different dynamic loading rates. On average, the loading plateau stress is 609 MPa for the 3% strain cycle and decreases to 537 MPa for the first 7% strain cycle. This decrease in the loading plateau stress is associated with localized slip due to continued cycling which assists the phase transformation. As can be seen in figure 39, there is a significant increase in the residual strain between the 0.5 Hz and 1.0 Hz loading rates. The residual strain measured after the fourth 7% strain cycle is 0.68% and 1.2% for the specimens loaded at 0.5 Hz and 1.0 Hz, respectively. Although the specimens show an increase in the residual strain values for higher loading rates, all

residual strain values remain below 1.4% providing good recentering capability even at strain rates equivalent to those associated with seismic events. Energy dissipation characteristics tend to be unaffected by the loading rate and remain too low to suggest the use of superelastic NiTi SMAs for purely damping applications. The dynamic tensile test results do suggest that NiTi wires can provide good recentering capability and some supplemental energy dissipation when used for seismic design and retrofit of building structures.

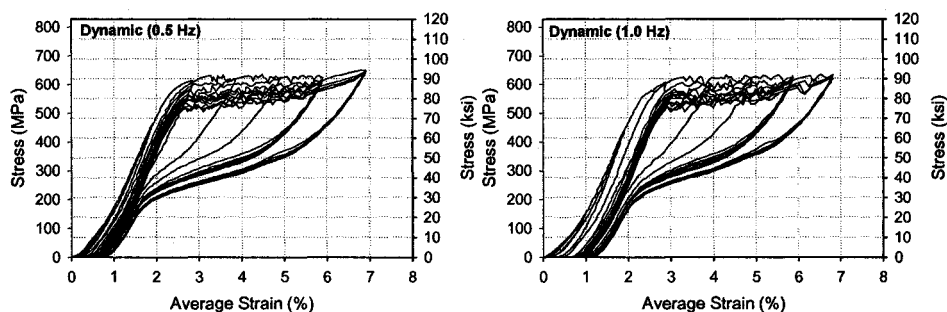


Figure 39 Stress-strain curves for the SMA wires tested at 0.5 Hz and 1.0 Hz

### 3.3 Small-Scale Braced Frame Test

Han et al. [79] studied the effectiveness of SMA braces to control a small scale two-story frame. Shake table simulations showed that the speed of vibration decay is faster for the SMA-controlled frame as opposed to the uncontrolled frame. Mao and Li [80] and Aizawa et al. [81] demonstrated through the use of shake table tests that frames with SMA-based energy dissipation devices, compared to uncontrolled frames, show greater potential to decrease the seismic response of a structure. Although many studies have shown promise for the use of SMA-based devices for seismic applications in buildings, most past research has focused on comparing their response to uncontrolled frames and has not looked at the benefits of using SMAs in comparison to other passive devices or

conventional systems used in steel frames. The aim of this section is to compare the response of a SMA braced frame to a steel braced frame in which both types of braces possess the same initial stiffness and approximately the same yield force in order to see how each bracing system affects the overall behavior of the frame.

### **3.3.1 Experimental set-up**

The reduced scale experimental set up is shown in figure 40. It includes a single bay frame structure, which is placed on a small-scale shake table. Accelerometers are attached to the shake table and at the top of the frame in order to provide feedback for the shake table control and to measure the top floor acceleration, respectively. The bay has a span of 31 cm and a height of 50 cm. The columns are made of 1.6 mm thick aluminum plates and the beams are made of 12.7 mm thick polycarbonate plates resulting in essentially rigid behavior for the beams. The natural period of the unbraced frame is 0.23 second. Two sets of additional mass, resulting in a 'low level' and 'high level' excitation for the braced frame, are placed at the top of the frame to cause a sufficiently large response in the frame to ensure the onset of the phase transformation and superelastic effect in the SMA wires. Relative displacements are used to measure the response of the frames and are computed by double integration of the absolute accelerations measured by the accelerometers attached to both the shake table and the top of the frame.

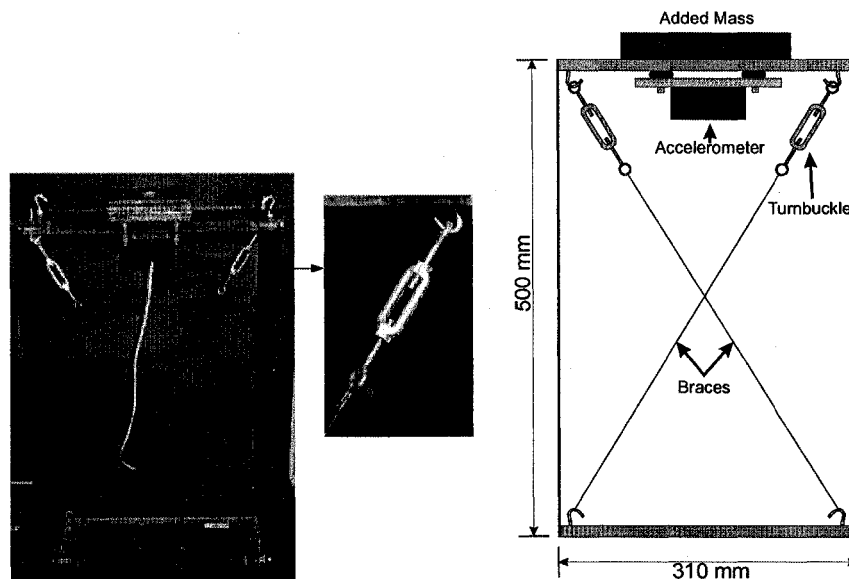


Figure 40 Experimental test setup and structure

The steel braces consist of a single soft-steel wire while the SMA braces consist of a short segment of superelastic NiTi wire (discussed previously) attached to a larger diameter length of steel wire (0.68 mm). Since the large diameter steel wire is much stiffer than the SMA segment, most of the deformation in the brace essentially takes place in the SMA segment. Only a portion of SMA wire is used in order to be able to control of the initial stiffness of the frame by adjusting the length of the SMA segment. Geometric and material properties for the two sets of braces are provided in table IV. Both types of braces are attached to the frame by metal hooks which are screwed into both the bottom and top floor of the frame as can be seen in figure 40.

Table IV  
Geometric and material properties of the two types  
of braces

Properties	Steel	SMA
Elastic Modulus, E (MPa)	200000	27000
Diameter (mm)	0.3556	0.2540
Area (mm <sup>2</sup> )	0.0993	0.0507
length (mm)	415	30
<b>Stiffness, K (N/mm)</b>	<b>47.9</b>	<b>45.6</b>
Yield Stress, $\sigma_y$ (MPa)*	276	593
<b>Yield Force F<sub>y</sub> (N)</b>	<b>27.4</b>	<b>30.0</b>

\*For the SMA, *yield stress* is indeed the martensite start transformation stress.

In order to compare the behavior of the steel and SMA bracing systems, the structures are subjected to the North-South component of the 1995 Kobe earthquake recorded at the Japanese Meteorological Agency Station in Kobe, Japan, scaled in both time and magnitude to provide the correct accelerations on the reduced scale shake table. The two different levels of additional mass are applied to the frames. The first amount of additional mass is approximately 0.48 kg which produces the ‘low level’ excitation, which does not lead to yielding of the steel braces. In the second case, an additional mass of approximately 1 kg is used which produces the ‘high level’ excitation and results in yielding of the steel braces.

### 3.3.2 Experimental results

Figure 41 shows the displacement time history of the top of the frame for the ‘high level’ excitation specimen with either SMA braces or steel braces. The displacement corresponding to brace yield for the steel braces and onset of the phase transformation for the SMA braces is approximately 1.25 mm. For the ‘high level’ excitation, the first six seconds of the earthquake response show similar behavior for the steel and SMA bracing systems. Thereafter, yielding occurs in the steel wires and the roof displacement

of the steel braced frame becomes large with a maximum roof displacement of 37.5 mm. For the SMA braced structure, the maximum roof displacement is only 7.6 mm resulting in an 80% reduction in the roof displacement as compared to the steel braced frame. The displacement time history clearly shows a faster attenuation of the response when the SMA braces are implemented. These results underline the advantage of using SMAs for seismic control since the SMAs do not accumulate residual strain and thus one brace is always engaged where the steel braces can go slack as a result of permanent deformation. In addition to always passing through the origin, the SMA braces can accept large strain values resulting in greater control and a more rapid decrease in the response of the structure even with a high acceleration input.

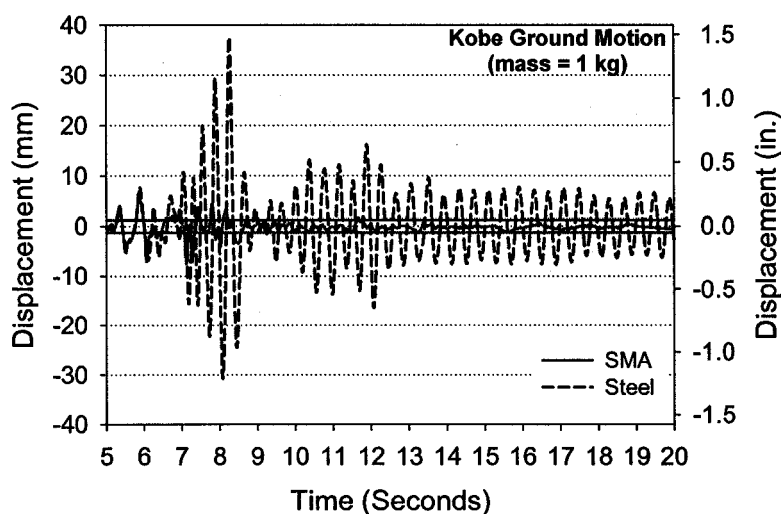


Figure 41 Displacement time history of steel braced and SMA braced frames subjected to the Kobe ground motion (mass = 1 Kg) with the displacement to cause yield in the braces marked by the horizontal solid lines



### 3.4 Analytical Verification Study

The experimental shake table and uniaxial tensile material results can be used to verify an analytical model of the small scale braced frame with either steel or SMA braces. A good model which allows for monitoring of the forces in the braces during an earthquake can provide details of the stresses encountered by both the braces and their connections which can aid in the design of new systems. Many researchers have used numerical models to predict the response of SMA braced structures with particular attention being paid to the modeling of the SMA behavior [79;82;83]. Andrawes et al. [84] found that the response of a structure is insensitive to the type of phenomenological model used to describe the cyclic behavior of the SMAs. The main objective of this section is to validate the finite element model (FEM) of the braced frame and compare the results to those found during the experimental shake table test. To this end, two different multi-linear models are used to represent the cyclic behavior of the superelastic SMAs. The first model considers internal hysteretic cycles (sub-cycles) as purely elastic through the hysteresis and is called the elastic sub-cycle model. The second model generates the sub-cycles by an elastic unloading until an instability (trigger) line is reached, followed by an unloading aimed toward a return point. Internal hysteretic loading is approached in a similar manner with the instability line marking the start of the loading plateau. This type of model is extensively studied in a work by Thomson et al. [85]. It has been shown that through the use of an instability line, the actual small strain level cycle behavior is better captured as the reverse transformation tends to occur at higher stress or force levels. Given the greater accuracy in capturing the actual cyclic behaviour and the lack of increased computational time, this model is included in this study and is herein referred to as the trigger-line model. Schematics of the two models are shown in figure 42.

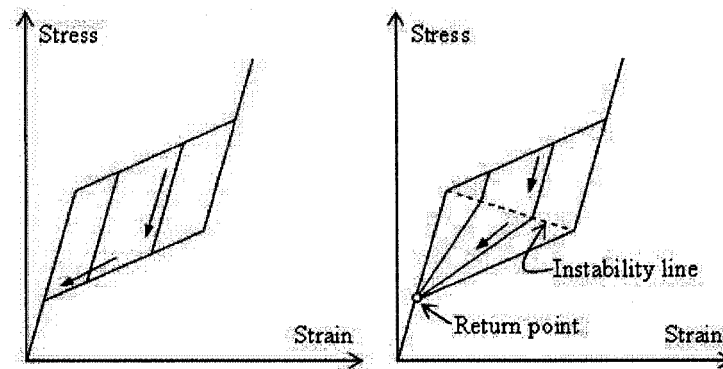


Figure 42 Multi-linear models used to represent the cyclic behaviors of SMAs. Left: Elastic sub-cycle model. Right: Trigger-line model

### 3.4.1 FEM approach

The simulations are carried out using the general-purpose finite element software ANSYS 8.0. [8], which is chosen for its ability to define material models via a user programmable subroutine. Different analysis options such as contact detection, sub-modeling, and solid elements can be useful for future investigation.

A multi-linear model is used to describe the superelastic behavior for both models via the USERMAT subroutine. The properties are based on a 7% strain cycle from the 2 Hz dynamic uniaxial tensile test of the NiTi wires previously discussed (Figure 43). Since the wires were only tested up to approximately 6.5% strain and still had not reached the fully stress-induced martensite phase, a strain of 8% is assumed as the end of the martensitic phase transformation. During the small shake table tests, the SMA wires are mechanically trained to stabilize their properties before the test is run. As a result, the model assumes that no further accumulation of residual strain will occur [61].

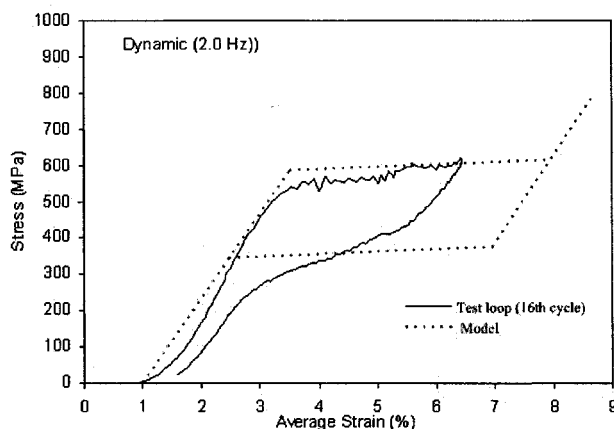


Figure 43 Comparison of the experimental hysteretic loop (2 Hz, 16th cycle) with the multi-linear model used for the analytical calculation

Shell elements are used to represent the columns, base, and top floor of the frame as can be seen in figure 44. The small size of the structure allowed for such detailed modeling without a large increase in computational time. A mass element at the top floor of the frame simulates the additional mass in the experimental model used to create either the 'high level' or 'low level' excitation. The connection between the braces and the floor system is modeled with beam elements while the steel braces are modeled with tension-only spars elements and tension-compression spars elements are used to account for the turnbuckles. The SMA brace behavior is applied through a link element with user programmable capabilities. In order to determine the appropriate damping ratio to apply to the analytical model, a free decrement test is performed on the experimental structure. The results showed that 2% Rayleigh damping for the first mode is necessary to obtain similar free decrement results between the experimental and analytical models. A full transient time history analysis using the North-South component of the Sylmar County Hospital Parking lot motion recorded during the 1994 Northridge earthquake is performed to validate the model. Both the elastic sub-cycle and trigger line models for the SMA behavior are evaluated.

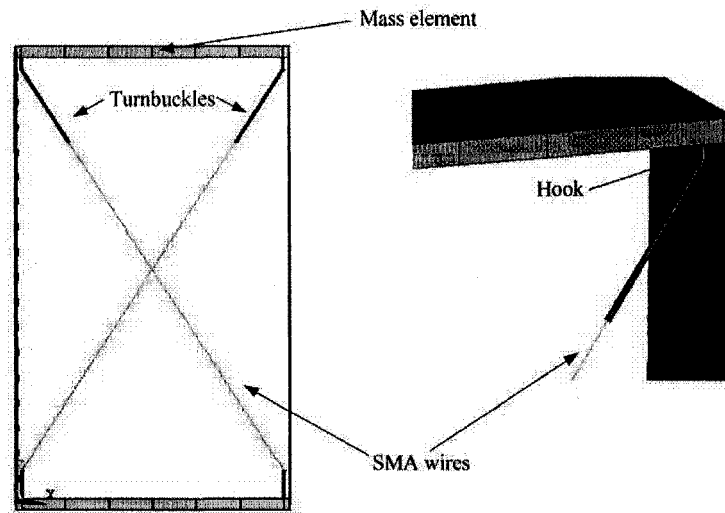


Figure 44 Finite element model of the single story frame

### 3.4.2 Results of the simulations

Experimental and analytical displacements of the SMA braced frame are illustrated in Figure 45. The results show the experimental and analytical displacement time history for the SMA braced structure where either the purely elastic sub-cycle SMA model or the trigger-line SMA model is used in the FEM. The displacements obtained from the experiment and analytical studies are in good agreement in terms of both magnitude and frequency of the response. The peak displacements are 26.5 mm, 27.3 mm, and 29.4 mm for the experimental, elastic sub-cycle model, and trigger-line model, which is only a 3% and 11% difference between the experimental results and those for the two analytical models, respectively. These results suggest that the FEM does a good job at capturing the response of the single-bay frame implementing SMA braces. A comparison of the two analytical models shows that both are in good agreement with the experimental results and suggest that either model can be used to adequately capture the response of the structure under typical earthquake loadings.

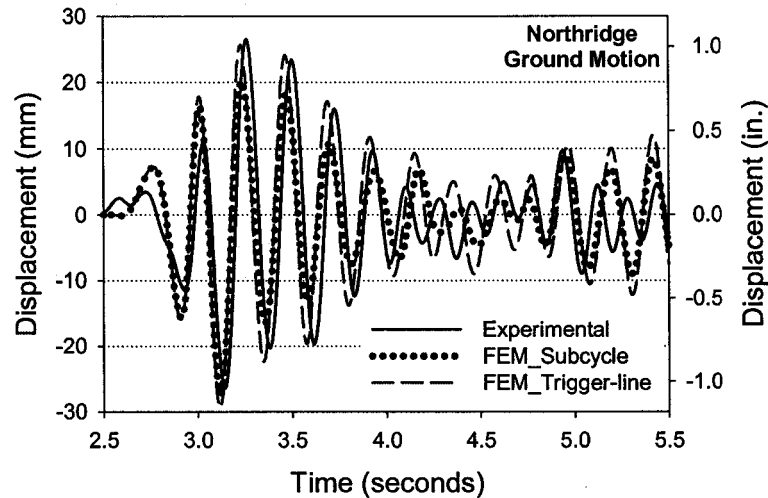


Figure 45 Comparison of the experimental and analytical displacement time histories of the structure subject to the Northridge ground motion

### 3.5 Pre-Straining SMA Bracing System

Past results and those from this current study have shown the ability of SMA based devices to reduce the seismic response of structures. Recently, some researchers have suggested that the use of pre-strained SMAs in devices can be beneficial and provide a means by which the SMA always acts in tension. Dolce and Cardone [19] and Dolce et al. [20] proposed pre-straining the SMAs to approximately 3.5% strain for their device. As a result, the wires are always stressed in tension causing a wide hysteretic loop and an apparent threshold force. Aizawa et al. [81] studied the application of SMAs as an energy dissipation device in a six-story steel frame. The authors used a pre-strain level of 2.75% for the SMA wires. Shake table tests revealed that the device significantly reduced the energy consumption of the frame itself due to the increase in energy dissipated by the braces. Saadat et al. [83] used a single degree of freedom model to analytically investigate the feasibility of developing energy absorption mechanisms based on SMA behavior and found that pre-straining the SMA wires has a noticeable

impact on the response of the structure. In a similar study to this current one, Aiken et al. [86] proposed a NiTi wire bracing system with both no pre-strain and a variety of pre-strain values between 2.5% and 6.0%. This study is one of the earliest to look at different pre-straining values, but does not take an in depth look at the optimal pre-straining level and the effect that various pre-strain levels have on the energy dissipation capacity of the SMA braces. Although these past studies have suggested that pre-straining the SMAs can be beneficial, none concisely analyze the effect of different pre-straining levels on the response of a structure to several different ground motion records. Many of these past cases cycled between predetermined strain levels or only pre-strained the SMAs to a single level in order to ensure tension-only superelastic behavior. As of yet, no trends in the response of structures with respect to SMAs pre-strained to various levels have been identified.

### 3.5.1 Analytical pre-stain model validation

In order to address the lack of knowledge associated with pre-straining SMAs used for seismic design and retrofit of building structures, both experimental and analytical studies are performed on the same frame, which has been presented previously, with the SMAs being pre-strained to various levels. By pre-straining the SMA wires, the SMA braces have already reached their loading plateau as can be seen in figure 46. As a result, the SMA braces undergo hysteretic sub-cycles immediately upon engaging and provide added energy dissipation to the structural system. The experimental SMA braces are pre-strained by shortening the turnbuckle up to a given distance to apply a predetermined level of deformation (representing a given strain level) to the SMA cables. For the analytical study, pre-strain values are applied to the model via a temperature variation on the turnbuckles, according to Eq. (3.1):

$$\varepsilon = \alpha \cdot \Delta T = \frac{\Delta l}{l_i} \quad (3-1)$$

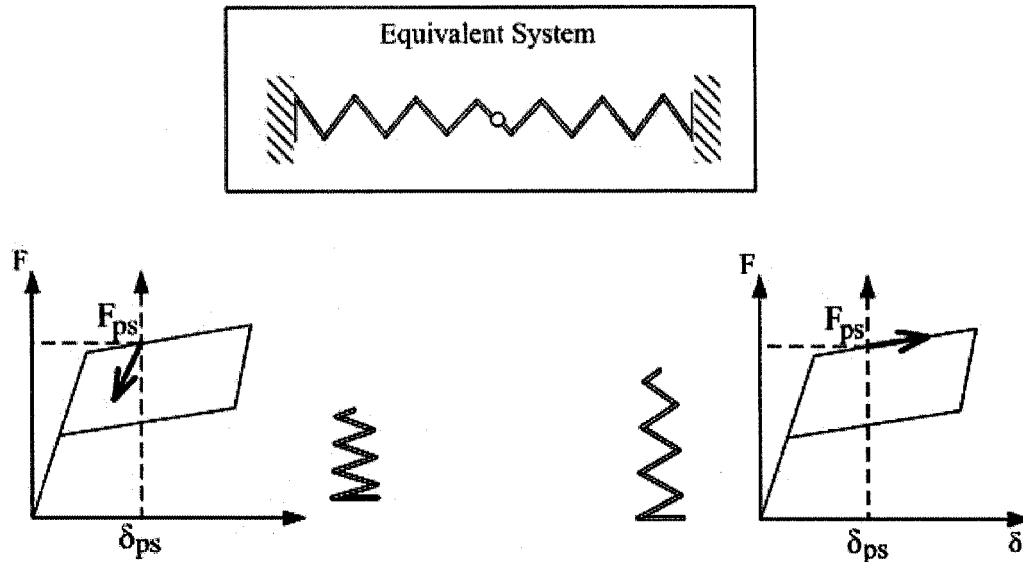


Figure 46 Conceptual equivalent system of springs with the stress-strain behavior being shown when pre-straining is used

Where  $\varepsilon$  is the strain increment,  $\alpha$  is the thermal dilatation coefficient (for this study  $\alpha = 1$ ),  $\Delta T$  is the temperature variation applied to the turnbuckles,  $\Delta l$  is the resulting change in length of the turnbuckle, and  $l_i$  is the initial length of the turnbuckle.

As an initial part of the pre-straining study, the ability of the SMA analytical models to capture the behavior of the structure undergoing the previously presented Northridge ground motion when the braces are first pre-strained to either 1% or 4% is evaluated. Figure 47 provides the experimental and analytical displacement time histories for the 1% pre-strain case where both the elastic sub-cycle and trigger-line SMA models are utilized. The ability of the analytical model to predict the experimental results tends to decrease with an increase in pre-straining value. For the 1% pre-strain case, the difference in maximum displacement found experimentally and analytically using the elastic sub-cycle and trigger-line model are approximately 12% and 8% with difference of 20% and 1.4% for the 4% pre-strain case, respectively. The ability to capture the frequency of the displacement time history is also effected by applying a pre-strain value

to the SMA braces. The results suggest the need of further investigations into the material behavior of pre-strained SMAs in order to develop more accurate material models for cases when pre-strained SMAs are implemented into seismic design and retrofit applications. However, the models presented reasonably predict the maximum displacement.

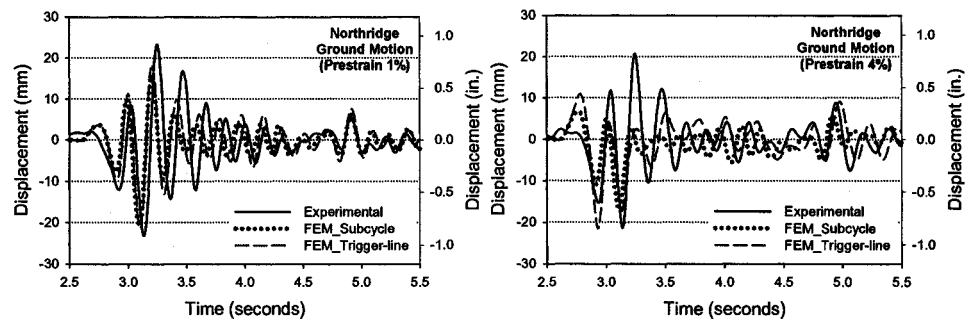


Figure 47 Comparison of the experimental and analytical displacement time histories of the structure subject to the Northridge ground motion with braces pre-strained to 1% and 4%

As a result of these initial pre-strain tests, four different hypotheses can be formulated to explain the effect of using pre-strained SMA braces on the response of the structure:

- (i) Increased energy dissipation is obtained as the sub-loops cover a larger area when starting from a non-zero strain position ( $\delta_{ps}$  in figure 46).
- (ii) For the majority of the ground motion, the braces are stressed in tension assuring that both of the wires are always engaged and providing a means of controlling the response of the structure.
- (iii) The stiffness is variable depending on the initial pre-strain level. High initial stiffness is obtained for low pre-strain levels while low initial stiffness is obtained when pre-straining causes an initiation of the phase transformation. A low stiffness structure tends to show larger displacements.



- (iv) Pre-tensioning the braces creates a re-centering force  $F_{ps}$  that tends to stabilize the structure. The equivalent system can be idealized by two springs in series working in opposition (top of figure 46). When a displacement is applied to the structure and the threshold re-centering force is reached, one cable undergoes the forward transformation, while the other undergoes the reverse transformation. The instantaneous resulting force is then the difference of the two tension forces in the springs.

In order to test these hypotheses, an in-depth experimental and analytical study on how the pre-straining level affects the response of the structure is undertaken for three different ground motions.

### 3.5.2 Pre-strain level study

Shake table tests are performed to study the effect that pre-straining the SMA braces has on the response of the frame. The previously presented Kobe and Northridge ground motions along with the North-South component of the 1940 El Centro ground motion measured at the Imperial Valley Irrigation District Substation have been chosen for this purpose. The same single-story frame presented previously is considered for this study with the exception that the braces are entirely made of SMA wire and the turnbuckles are used to apply the pre-strain values. Additional masses of 2 kg for the El Centro ground motion, 0.59 kg for the Northridge ground motion, and 0.59 kg for the Kobe ground motion are added to the roof of the structure to ensure adequate elongation of the braces. The results from the El Centro ground motion are presented in detail to summarize the effects of pre-straining on the structures response. The displacements time history for the top floor of the frame undergoing the El Centro ground motion is shown on figure 48 for the four different pre-straining levels. The maximum displacements for the 0%, 1%, 2%, and 4% pre-strain levels are 17.2 mm, 7.7 mm, 8.8 mm, and 10.3 mm, respectively.

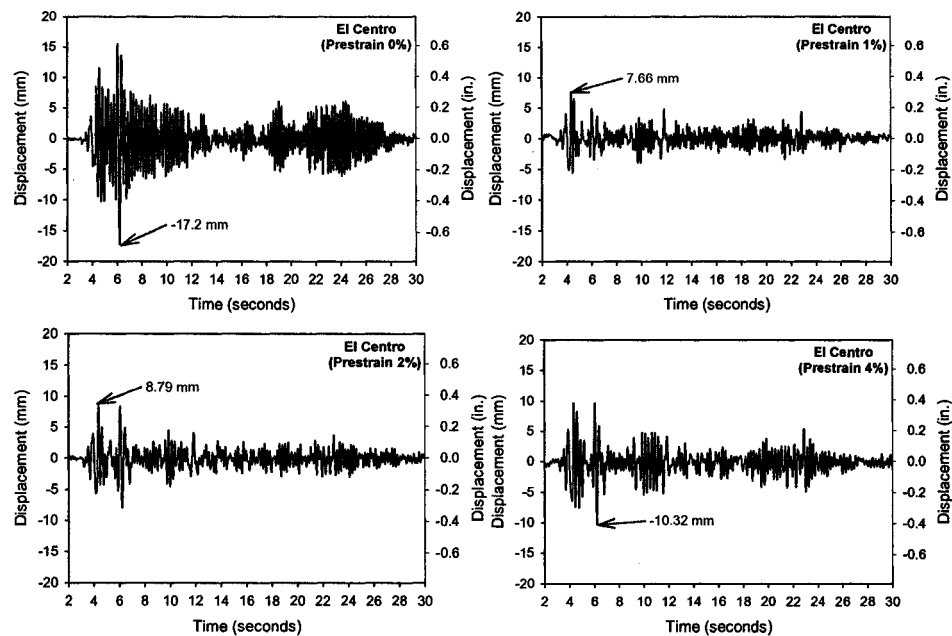


Figure 48 Time history displacements (mm) of the structure subject to El Centro ground motion for different prestrain values

Since instrumentation for the experimental study consisted of accelerometers, only a limited amount of data can be obtained in regards to the response of the structure and behavior of the braces. Also, as previously mentioned, the analytical model of the braced structure does not accurately predict the behavior of the frame seen experimentally when pre-straining is used. For these reasons, a more detailed look at the brace behavior is obtained using the analytical SMA elastic sub-cycle model by considering the geometric relationship between movements of the top floor and stretching of the braces from the experimental results. The computed experimental time history of the elongation of the braces is then applied as a displacement time history to only the SMA model (without considering the rest of the frame) in order to determine the stress-strain relationship which the braces underwent during the experiment. Figure 49 through 51 show the results of this analysis for the El Centro ground motion for each of the four pre-strain levels.

The stress-strain results for one of the SMA braces due to the El Centro ground motion are shown in figure 49 for four different levels of pre-strain. For the cases where no pre-strain is applied and only 1% pre-strain is applied to the braces, the stress-strain curves start along the initial elastic curve which results in a significantly stiffer structure during the initial loading. As a result, strain levels in the braces are significantly smaller as compared to those braces which are pre-strained at higher levels. The maximum strain reached in the brace for the 0% and 4% pre-strain cases are 3.1% and 5.9%, respectively. A further consequence of starting along the initial elastic curve is the lack of hysteretic behavior during the initial loading cycles which limits the amount of supplemental energy dissipation provided. The 2% and 4% pre-strain cases show much larger hysteresis values suggesting that not only will the recentering capability of the SMAs help control the response of the structure, but larger values of supplemental energy dissipation are also provided.

A comparison of the energy dissipated by the SMA braces for the different pre-strain levels as a result of the El Centro ground motion is provided in figure 50. The results show that a larger amount of energy is dissipated when the SMA braces are first pre-strained to a level which places them along the loading plateau of the stress-strain curve. Two to three times the energy dissipation capacity of SMA braces that are not pre-strained can be obtained by pre-straining the braces above 2% strain. Although, it should be noted that the energy dissipated by the superelastic SMA braces still remains low compared to other passive energy dissipation devices suggesting that the reduction in the response can be attributed mostly to the recentering capacity of the SMAs.

The notion that the SMA braces will remain in tension due to the application of pre-straining, resulting in a better performance of the structure, can be verified through the stress time history of the braces shown in figure 51 as a result of the El Centro ground motion. The results show that when the SMA wires are not pre-strained, they experience negative stress values (compression) at several points and do not provide any structural

control. For the cases in which the SMA wires are first pre-strained, there exist very few instances where the braces experience negative stresses. At higher pre-strain levels, the braces do not undergo compression and are always engaged.

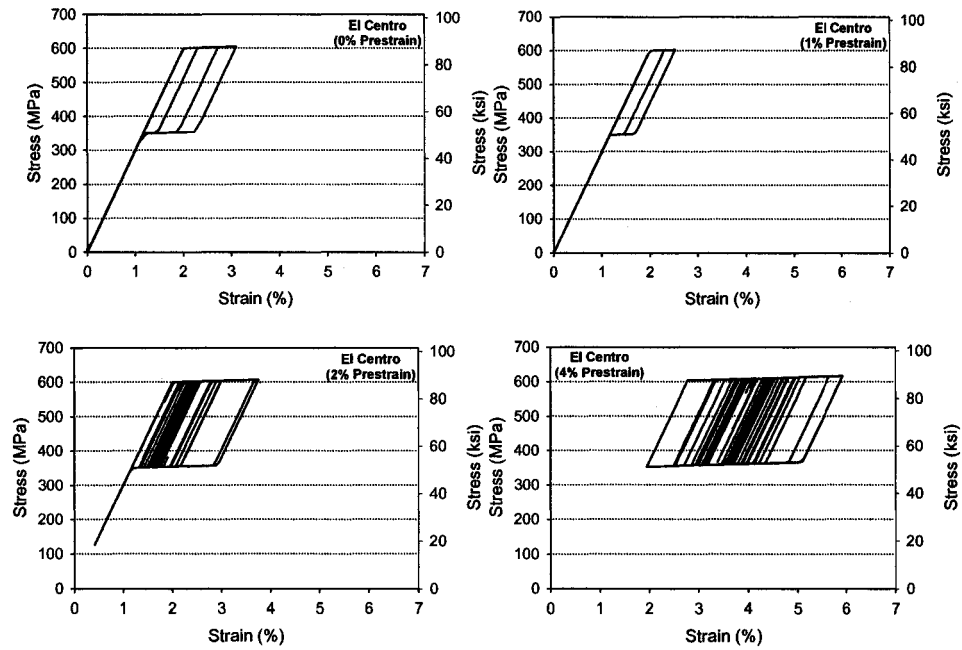


Figure 49 Stress-strain diagram of the two cables subject to El Centro ground motion for different prestrain values

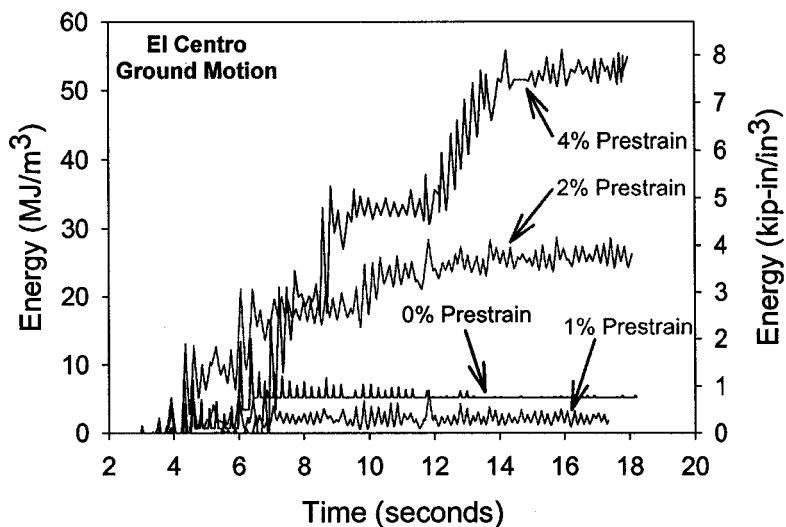


Figure 50 Energy consumption of the two cables subject to El Centro ground motion for different prestrain values

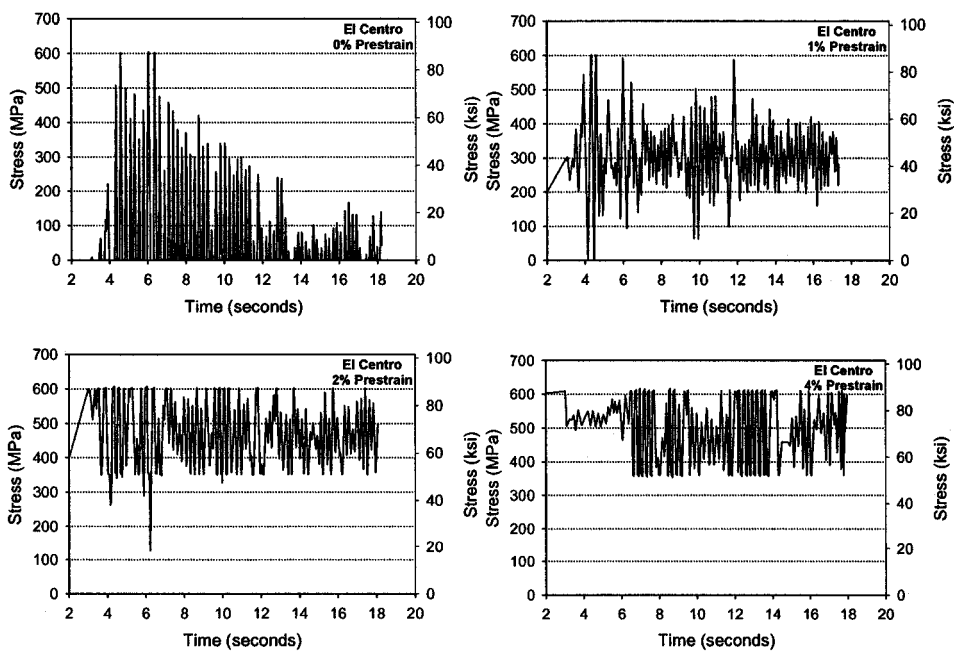


Figure 51 Stress history of the two cables subject to El Centro ground motion for different prestrain values

### 3.5.3 Discussion on the pre-strain effect

Figure 52 shows the normalized maximum displacements of the top floor of the frame for the three different ground motions when the SMA braces are pre-strained to different strain levels. The average maximum displacement for the case where the braces are not pre-strained is 21.8 mm and decreases to 15 mm, 16 mm, and 17.6 mm when the SMA braces are pre-strained to 1%, 2%, and 4% strain, respectively. For each ground motion, pre-straining the SMA braces to any level results in a decrease in the response compared to the zero pre-strain case.

The increase in maximum displacement when going from pre-strain levels of 1% to 4% for the El Centro and Kobe ground motions and from pre-strain levels of 2% to 4% for the Northridge ground motion can be attributed to changes in the stiffness of the structure due to the onset of the phase transformation when strained at or above 2% strain. When the SMA braces are only pre-strained to 1%, they remain on the initial elastic curve upon initial loading rather than on the loading plateau resulting in a stiffer initial structure with both braces being engaged and having this same higher initial stiffness. This increased initial stiffness can help to reduce displacements in the structure when the ground motion has large magnitude accelerations early in its time history. It is clear that applying some pre-strain to the SMA braces does act to reduce the response of the structure and increase the speed of attenuation of the structure's displacement over time.

For the three ground motions, it can be noted that the displacements are almost the same for the 2% and 4% pre-strain levels. This observation is in agreement with the notion that the recentering force helps to stabilize the structure and reduce displacements during a seismic event. This can be suggested since the forces for those pre-strain levels are similar because both pre-strain levels place the SMA braces in the loading plateau portion of the stress-strain curve. However, the re-centering force level differs for the

1% and 2% (or 4%) pre-strain levels. As a result, the decrease in maximum displacement is attributed to a stiffness change previously discussed.

A further consequence of starting along the initial elastic curve is the lack of hysteretic behavior during the initial loading cycles which limits the amount of supplemental energy dissipation provided. Figure 53 suggests that the amount of supplemental energy dissipation due to the flag-shape hysteretic behavior of the SMAs tends to increase with increased levels of pre-strain. This can be attributed to the fact that by pre-straining the SMA braces most of the behavior occurs along the hysteresis loop rather than along the initial elastic portion of the stress-strain curve. Although the energy dissipated increased with an increase in pre-strain level, the maximum displacements did not significantly decrease. The energy dissipation associated with the Kobe ground motion increased by 133% when the SMA braces were pre-strained to 4% as opposed to 2% strain, but the maximum displacement increased slightly. These results suggest that the energy dissipation is only a minor component in controlling the response of the frame with SMA braces.

Based on these findings, it is suggested that pre-straining in the range of 1.0-1.5% can provide the optimal level of structural control in most cases. When pre-straining to higher values, the possibility of fracture due to the development of large strains in the SMA braces has to be carefully evaluated. Further, relaxation in the SMA braces over time has to be taken into consideration. Dolce et al. [20] tested a pre-strained SMA cable over a period of three weeks and found that the effect of relaxation in the SMAs is negligible. However, because earthquakes are scarce events, further research is needed over a longer period of time. The effects of seasonal actions on the properties of the SMAs also must further be understood before implementing pre-strained SMA braces into practice [39].

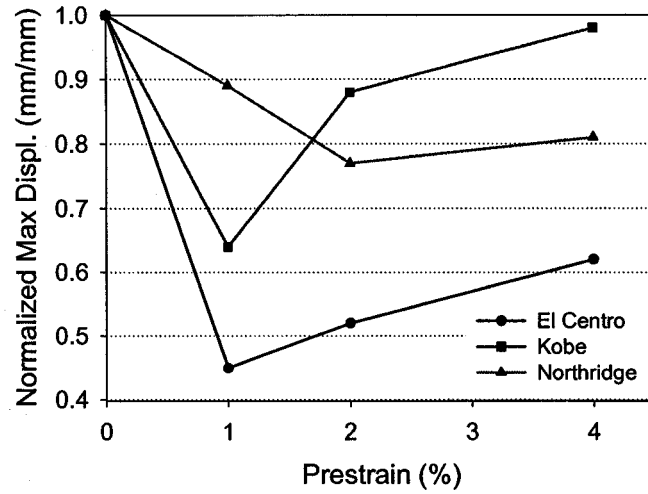


Figure 52 Normalized maximum displacement obtained for different pre-strain values

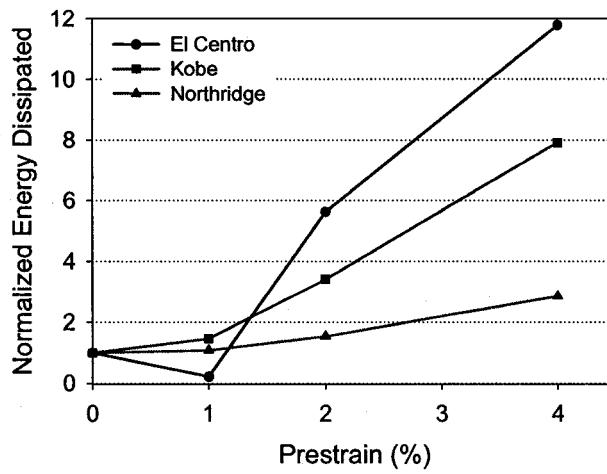


Figure 53 Normalized energy dissipated for different pre-strain values



### 3.6 Conclusion

In this paper, the effectiveness of using SMA braces to control the response of a single-bay frame during a seismic event is investigated. The response of a steel braced structure is compared with that of a SMA braced structure in which the braces possess the same stiffness and yield force. Shake table tests are conducted and show that the SMA bracing system provides a consistent reduction in the response due to the re-centering capability associated with the material.

The second goal of this study is to develop a FEM of the single-bay braced structure and to compare the performance of this model to the experimental results when two different SMA sub-cycle models are considered. The results obtained with the use of the trigger-line SMA model are slightly better than those obtained with the purely elastic sub-cycle model. The differences between the experimental and analytical results are minimal when no pre-straining is applied to the braces. The comparison shows difference in both magnitude and frequency of the displacement time history when pre-straining is applied suggesting that further investigation into analytical models of SMA behavior which can handle pre-straining needs to be undertaken.

The effect of pre-straining the SMA braces on the response of the single-story frame is also investigated. Shake table tests confirm that by pre-straining the SMA braces the maximum frame displacement can be reduced. The stiffness variation and the fact that the braces remain in tension when they are pre-strained to different levels have been identified as the key factors resulting in this reduction. Although the energy dissipated increases considerably with increased pre-straining, this factor has been identified as a secondary factor for the reduction of displacements. The experimental results show an interaction between the four hypotheses identified earlier and a dependency on the ground motion used. Finally, it is found that an optimal pre-straining level exists in the range of 1.0-1.5% pre-strain.